Lake energy balance response to 21st century warming in the tropical high Andes

Jarunetr (Nadia) Sae-Lim[a],*, Bronwen L. Konecky[a], Carrie Morrill[b], Neal Michelutti[c], Christopher Grooms[c], John P. Smol[c]

[a] Department of Earth, Environmental, and Planetary Sciences, Washington University, USA

[b] National Centers for Environmental Information, National Oceanic and Atmospheric Administration, USA

[c] Paleoecological Environmental Assessment and Research Lab (PEARL), Department of Biology, Queen's University, Canada

*Corresponding author: Jarunetr Sae-Lim, Now at: Department of Earth System Science, University of California, Irvine, 3200 Croul Hall Irvine, CA 92697. Email: nsaelim@uci.edu

Abstract

The response of Andean high-alpine lakes (>4000 m above sea level) to atmospheric warming is poorly understood, in part due to a lack of long-term limnological and meteorological observations. Here, we use *in situ* observations, reanalysis data, satellite-derived data, and climate modeling output data paired with a one-dimensional lake energy balance model to investigate the response of lake thermal properties to observed and projected 21st century warming in the tropical high Andes of Peru. The lake model configuration is based on Lake Sibinacocha (13.86°S, 71.02°W, 4860 m a.s.l.), the largest high-alpine lake in the Andes and one of the few such lakes with temperature observations sufficient for model calibration. Relationships between recent air and lake temperature changes were investigated using the model forced with 21st-century ERA5-Land climate reanalysis data, CERES satellite-based observations, and future relationships were investigated using two CMIP6 future climate

scenarios with CESM2 (SSP2–4.5 and SSP5–8.5). Results show that Sibinacocha whole-lake average temperature stayed relatively consistent between 2000 and 2023 due to high interannual variability. Lake Sibinacocha temperatures also display interannual variability that aligns with air temperature variations, suggesting that broad climatic teleconnections that affect Andean air temperatures also influence lake temperature and stratification. Under the SSP2–4.5 and SSP5–8.5 scenarios, the model indicates an acceleration of Lake Sibinacocha's whole-lake warming rate. By 2091–2100, Lake Sibinacocha is projected to increase 2.5 °C to 5.9 °C. Lake Sibinacocha is projected to warm unevenly, with greater warming in the top 20 m and austral spring, contributing to increased weak stratification in spring. Lake Sibinacocha is anticipated to respond more slowly to warming simply due to its large size. Therefore, our results should be considered a conservative end-member for other lakes in the tropical high Andes, which, due to their shallower sizes, will likely respond more quickly to atmospheric warming.

Keywords

Lake energy balance modeling, Lake temperature, South America, Tropical Andes, Climate change, high elevation warming

Highlights

- Sub-seasonal to seasonal lake thermal properties are well simulated by 1-D lake energy balance model.
- High interannual temperature variability at Lake Sibinacocha overwhelms any possible warming signal from 2000-2023.
- The whole-lake warming rate will accelerate mid-century under SSP2-4.5 and SSP5-8.5 scenarios.

- Sibinacocha is projected to warm unevenly, with greater warming expected in spring.
- Future warming will likely drive shifts in lake ecosystems throughout the Andes.

1. Introduction

The highlands (>4000 m above sea level; a.s.l.) of the Peruvian Andes host about 70 % of the world's tropical glaciers (Rabatel et al., 2013; Vuille et al., 2008). This region also provides freshwater to lakes and rivers supplying Andean communities as well as the Amazon basin (Buytaert et al., 2017; Vuille, 2014). For the last several decades, the tropical Andes have been warming significantly and are projected to further warm in the future (Urrutia and Vuille, 2009). This ongoing warming has caused glaciers and ice caps in this region to retreat substantially, including the world's once-largest tropical glacier – the Quelccaya Ice Cap in southeast Peru, which has been projected to disappear in the 2050s under some scenarios (Yarleque et al., 2018).

Lakes are among the world's most important natural resources as they store accessible freshwater, foster a high level of biodiversity and provide key ecosystem services (Heino et al., 2021). In general, warming can alter lake thermal structure and evaporation, which are important controls on lake biogeochemistry and ecology (Adrian et al., 2009; Woolway et al., 2022). Yet the magnitude and nature of these responses depend on regional climatic and lake characteristics including morphology, size, thermal properties, mixing regime, and trophic index (O'Reilly et al., 2015; Kraemer et al., 2015). Tropical alpine lakes share some thermal similarities to cool high-latitude lakes, but they are distinct in that tropical air temperatures exhibit a large diurnal cycle but only minimal seasonality (Labaj et al., 2018). Tropical alpine lakes also have a year-round growing season with no winter ice cover (Michelutti et al., 2020), distinct from high-latitude lakes. Recent ecological studies from the tropical high Andes imply that anthropogenic

warming has already altered lake ecosystems, including shifts in diatom assemblages and whole-lake production (Michelutti et al., 2015, 2020; Fritz et al., 2019; Benito et al., 2022). Most studies estimating future lake responses to climate change tend to focus on the northern hemisphere, the extratropics, and low elevations, thanks to both the high abundance of lakes situated there and the availability of lake temperature data for calibrating models (Woolway et al., 2021; Shatwell et al., 2019; Sahoo et al., 2013; Winslow et al., 2018; Woolway and Merchant, 2019; Kirillin, 2010). In the Southern Hemisphere and the global tropics, however, lake responses are not well-quantified, presenting a challenge to societal adaptation and conservation planning efforts.

In this study, we investigate how lake thermal properties correspond to past and future trends and variability in local air temperature using a 1-D lake energy balance model of Lake Sibinacocha, Peru (-13.86°, -71.02°; 4860 m a.s.l.), the largest high-alpine lake in the Andes. Lake Sibinacocha is a major freshwater source for many Peruvian communities, cities, and ultimately for the Amazon River, and it is a critical resource for local irrigation and hydroelectricity (Kronenberg et al., 2016). Located in the Cordillera Vilcanota, Lake Sibinacocha experiences relatively cold air temperatures all year with small seasonal variations. Like other tropical alpine settings, this region experiences strong solar radiation during the day and an extreme diurnal cycle (Hardy, 2019; Romatschke et al., 2010; SENAMHI, 2024). These features make tropical, high-elevation lakes difficult to compare to lake energy balance modeling studies from sites in the lower-elevation tropics or in the mid-to high-latitudes.

We first calibrate the energy balance model using a combination of climate reanalysis, climate model outputs, satellite-derived radiation data, and in situ observations. We then use the calibrated model to provide a baseline for early 21st century (2000 2023) lake temperature and

thermal structure and to project future changes (2015–2100) based on two radiative forcing scenarios adopted by the Intergovernmental Panel on Climate Change (IPCC) (Danabasoglu, 2019b, 2019c). Our work is the first lake energy balance modeling study to produce quantitative estimates of tropical Andean lake temperature under past and future warming.

2. Study site

The Cordillera Vilcanota is the second-largest glaciated range in Peru and hosts the Quelccaya Ice Cap, one of the world's largest tropical ice caps and a focus of glaciological, climate, and meteorological study since the 1970s (Hardy, 2019; Thompson et al., 2013; Thompson et al., 1994). The local ecosystem is classified as moist puna, a type of treeless and wet montane grassland found at high elevations (Baied and Wheeler, 1993). According to a weather station located near the southern shore of the lake, daily average December – February (DJF) and June – August (JJA) air temperatures of this site are 2.66 ± 0.25 °C and 1.04 ± 0.48 °C, respectively (January 2017 – December 2023; SENAMHI, 2024). Although seasonal temperature variation is small, diurnal temperature variation is extremely large, with night-to-day differences in temperature of up to 10.80 °C. The Cordillera Vilcanota receives most precipitation during the austral summer. The average DJF and JJA total precipitation are 396.6 ± 81.0 mm/season and 18.3 ± 17.3 mm/season, respectively.

Lake Sibinacocha is an ultra-oligotrophic (Table S1), glacial-fed lake with a length of 16 km and a surface area of 33 km^2. According to our bathymetric surveys (Section 3.1.1; Fig. 1c), the estimated lake volume is 1.7 km^3, with an average depth of 60.9 m and a maximum depth of 92.8 m. A dam was constructed at the outflow at the south end of the lake in 1988 and formally

inaugurated in June 1996 to increase the energy production of the downstream Machupicchu hydropower plant. This construction led to changes in the outflow seasonality (Bello et al., 2023). Before the dam was built, high lake outflows occurred from January to March, with a peak outflow of 6.0 m^3/s in January. In contrast, low outflows were observed from July to September, with a minimum outflow of 0.8 m^3/s in September. However, this pattern changed after 2002. High lake outflows were recorded from July to November, reaching a peak outflow of 6.27 m^3/s in September, while low outflows were seen from December to June, with a minimum outflow of 0.37 m^3/s in March (Bello et al., 2023). Nonetheless, the dam had minimal effect on Sibinacocha's lake level. Michelutti et al. (2019a) reported the presence of submerged archeological structures at a depth of ~3 m during the low stand in the 2017 field season. These structures were already submerged before the dam construction, as indicated by aerial photographs from 1931 (Shippee, 1991). Based on field observations in 2018, the lake level fluctuates about 2 m seasonally (Michelutti et al., 2019a).

Michelutti et al. (2019b) measured lake temperature-depth profiles at the north and south ends of Lake Sibinacocha (~11 km apart) and reported that Lake Sibinacocha is cold (mean annual surface temperature < 12 .C) and, despite its depth, experiences only short-lived periods of weak thermal stratification, and does not freeze. The thermal profiles of the north and south ends are coherent, suggesting that neither glacial meltwater flux nor artificial outflow regulation creates a substantial horizontal temperature gradient along the length of the lake. Michelutti et al. (2019a) also measured several small, shallow lakes near Sibinacocha, including Yanacocha (13.75 ha, 17 m deep max), Laguna 3 (26.95 ha, 10 m deep max), and Lado del Quelccaya (2.21 ha, 5 m deep max) (Fig. 1b). The annual average temperatures of these lakes vary slightly, but the seasonal cycle and intra-seasonal variability correspond well to that of Sibinacocha. Notably, Laguna 3

and Yanacocha are also classified as non-glacial lakes. The similarity in the thermal structures of Laguna 3, Lake Yanacocha, and Lake Sibinacocha supports the idea that the influence of glacial melt in the northern part of the lake and the outflow regulation in the southern part of the lake has minimal effect on the overall thermal structure of Lake Sibinacocha. However, it is important to note that only one year of data (September 2016 – August 2017) is currently available for comparison. The Sibinacocha watershed is home to some of the world's highest-altitude amphibian populations (Seimon et al., 2017), several vulnerable mammals (Doyle et al., 2003), and pre-Columbian archaeological features (Michelutti et al., 2019a). Thus, this study not only contributes to a better understanding of lake responses to climate change but also provides a solid ground for future ecological research at this site. Understanding the sensitivity of high alpine lakes to climate change is also useful for anticipating future tropical alpine lake properties and ecological changes, as well as informing conversations about possible adaptation strategies.

3. Methods

3.1. Input datasets

3.1.1. Lake bathymetry

Bathymetric surveys were performed at Lake Sibinacocha in August 2018 and May 2019 using a Humminbird Helix 7 CHIRP SI GPS G2N sonar device. The bathymetric data points of Lake Sibinacocha were interpolated using the natural neighbor interpolation method and mapped using ArcGIS Pro. To mark a boundary of the processed bathymetric map, we extracted a shoreline shapefile from Landsat 8 OLI/TIRS C1 Level-1 image (www.earthexplorer.usgs.gov) using ENVI software (Fig. 1c).

3.1.2. Limnological and meteorological data

Water temperature-depth profiles from the north and south ends of Lake Sibinacocha (Michelutti et al., 2019a; locations on Fig. 1b) were used to evaluate the performance of our model simulations. Methods are described in Michelutti et al. (2019a), but briefly: Temperature loggers were deployed at 0 m, 3 m, 6 m, 9 m, 12 m, 15 m, 18 m, 21 m, 24 m, and 27 m deep for the north end between August 21, 2017 to August 7, 2018 (351 days). For the south end, the water temperature data loggers were deployed at 0 m, 2.4 m, 4.9 m, 7.3 m, 9.8 m, 12.2 m, 14.6 m, 17.1 m, 19.5 m, and 21.9 m during two consecutive field seasons – from August 30, 2016 to August 15, 2017 (350 days) and from August 26, 2017 to August 11, 2018 (350 days). Temperatures were recorded every hour at each depth interval.

Meteorological data from two weather stations near Sibinacocha were used to correct biases in the input datasets used in our lake model (Table 1). Local hourly meteorological data, including air temperature, relative humidity, and wind speed, were obtained from an automated weather station located on the southern shore of the lake (4880 m a.s.l.) operated by Peru's national meteorological service (Servicio Nacional de Meteorología e Hidrología del Perú; SENAMHI). The period of available data coverage is March 2016 – December 2023, with a gap between May and July 2019.

3.1.3. Climate reanalysis data

We used the European Centre for Medium-Range Weather Forecast's (ECMWF) ERA5-Land hourly data from March 2000 to December 2023 (Muñoz Sabater, 2019) as model inputs in order to simulate past lake temperatures. We selected this dataset because the Cordillera Vilcanota exhibits a strong diurnal cycle, and the ERA5-Land hourly dataset contains diurnal cycle

information. Also, the ERA5-Land dataset was produced at enhanced spatial resolution (9 km vs 31 km in ERA5), making it more accurate than the ERA5 for land applications.

Five ERA5-Land variables including 2-m temperature (T2M), 2-m dew point temperature (D2M), surface pressure (SP), 10-m u-component of wind (U), and 10-m v-component of wind (V) were extracted from the ERA5-Land dataset at the grid point of -13.8° and -71.1°. The magnitude of the wind (i.e., wind speed) was calculated by taking the square root of the sum of the square of U and V. Relative humidity (RH) was calculated based on ERA5-Land's D2M and T2M following Lawrence (2005). Quantile-mapping algorithms were applied to correct biases of the ERA5-Land T2M, derived wind speed, and RH compared to respective observations, following previous studies with this lake energy balance model (Morrill et al., 2019).

3.1.4. Radiation data

The Clouds and the Earth's Radiant Energy System (CERES) Synoptic 1 degree Adjusted All-sky Profile Fluxes Surface Shortwave Flux Down and Longwave Flux Down from Terra+Aqua/NOAA20 Edition 4.1 between March 2000 and December 2023 at the grid point of -13.5° and -71.5° were used as the model's surface solar radiation downwards (SSRD) and surface thermal radiation downwards (STRD) inputs (Rutan et al., 2015). We chose this dataset because it is able to reproduce the diurnal and seasonal cycles of lake temperature, which are strongly affected by the amount of cloud cover and the relative proportion of shortwave to longwave radiation. According to this dataset, the mean annual surface shortwave radiation downwards and surface longwave radiation downwards are 205.44 ± 4.33 W/m^2 and 310.84 ± 2.77 W/m^2.

Although there are radiation observations from a nearby weather station (the Quelccaya Ice Cap; ~20 km from Sibinacocha horizontally; 5680 m a.s.l.; 2010–2012) and the ERA5-Land's SSRD and STRD (1981–2023), lake simulations generated using these datasets as model inputs and as a bias correction dataset show a persistent temperature lag relative to observations across all tunable parameters and published 1-D lake energy balance models (Supplementary information). The lag appears to arise from unrealistically low cloud amounts in these two datasets, which result in too much shortwave and too little longwave radiation as input to the lake model. Shortwave radiation penetrates deeper into the lake than longwave radiation, leading to greater heat storage at depth and a temperature lag in the model compared to lake temperature observations. Thus, neither the Quelccaya Ice Cap observed radiations nor the ERA5-Land radiations are appropriate for our lake energy balance modeling study.

3.1.5. Climate model experiments

To simulate future lake temperature (2015–2100) at Lake Sibinacocha, climatic data inputs were obtained from Community Earth System Model v2 experiments under shared two socioeconomic pathways (SSP) from the Coupled Model Intercomparison Project 6 (CMIP6). Specifically, SSP2–4.5 ("Middle of the road" scenario) and SSP5–8.5 ("Fossil fuel development" scenario) were selected to represent future medium and extreme human-induced climate change scenarios (Danabasoglu, 2019b; Danabasoglu, 2019c). The historical experiment (1850–2014) was used as a reference for our study (Danabasoglu, 2019a). Three ensemble members (r4i1p1f1, r10i1p1f1, and r11i1p1f1) were used for each experiment. Daily variables were extracted from these three experiments (except surface pressure which was only available at a monthly timestep). The delta method was applied to the CMIP6 outputs to bias correct relative to the quantile-mapped ERA5 Land dataset and downscale the CMIP6 outputs to hourly timestep for the lake energy balance

model. To do so, the quantile-mapped ERA5-Land and CERES radiation data were averaged across years to get an hourly climatological record for each variable between 2000 and 2014. The CMIP6 historical dataset was averaged across years to get a daily climatological record between 2000 and 2014. The scaling factors or "delta" was calculated by subtracting (dividing) each future projection from the historical climatology for T2M (RH, Wind, SSRD, STRD, and SP). Then these scaling factors were applied to the quantile-mapped ERA5 Land hourly averaged climatology record to get the inputs for the lake energy balance model following Morrill et al. (2019) and Dee et al. (2021). Due to the nature of downscaling, this correction method assumes that all hours of the diurnal cycle will change equally in the future.

3.2. Lake energy balance model

3.2.1. Model description

We calculated modeled lake temperatures and lake evaporation using the one-dimensional (1-D) lake energy-balance model of Hostetler and Bartlein (1990) as modified by Morrill et al. (2019). This model is governed by physically-based equations for energy transfer between the lake surface and overlying atmosphere, penetration and absorption of solar radiation at depth in the lake, and vertical redistribution of heat within the lake through mixing. The components of the lake surface energy balance are downwelling absorbed shortwave and longwave radiation, longwave radiation emitted by the lake surface, sensible and latent heat fluxes, and the vertical transfer of heat to/from deeper levels of the lake. Heat is transferred vertically in the lake via a parameterization for eddy diffusion and via density-driven mixing (convective overturn). The

lake temperature output is a result of the net change in the amount of heat stored in the lake per unit area and unit time.

Model inputs include climatic data and site-specific geographic and lake morphometric parameters. Climatic inputs were extracted from ERA5-Land's SP, quantile-mapped T2M, derived RH, and derived wind speed, and CERES's SSRD, and STRD at hourly frequency. We specified nine site-specific geographical and lake morphometric parameters in the lake energy balance model: latitude, longitude, local time relative to Greenwich Mean Time, the area of catchment and lake, maximum number of lake layers, lake area by depth from top to bottom, neutral drag coefficient (CDRN), shortwave extinction coefficient (ETA), and multiplication factor of eddy diffusivity for deep lakes (MIXFACT). Area of the catchment was determined by manual delineation of the drainage network based on ASTER Global Digital Elevation Model V003 (www. earthexplorer.usgs.gov) using ENVI. Lake area was highlighted using the band combination technique on Landsat 8 and then calculated using Region of Interest tool from ENVI. Our study does not account for lake water balance (e.g., glacial meltwater inflows and lake water outflows) as streamflow and temperature measurements of the meltwater streams and long-term local precipitation observations are unavailable at this site.

ETA has an inverse relationship with water clarity which can be estimated in the field using a Secchi disk (Kalff, 2002). CDRN is a parameter used in the bulk aerodynamic formulation of latent and sensible heat transfer, and depends on wave properties (e.g., wave age and height) that generally relate to lake-specific properties such as fetch (e.g., Gao et al., 2012; Subin et al., 2012). The turbulent mixing scheme is from Henderson-Sellers (1985), which parameterizes wind-driven mixing. Previously, researchers have noted that the Hostetler lake model tends to underpredict turbulent mixing in deep lakes, leading to insufficient heat loss in winter and

excessively fast warm-up in spring (Martynov et al., 2010; Subin et al., 2012). To adjust for this bias, these researchers have relied on either (1) increasing the eddy diffusivity values by factor 1–1000 (Martynov et al., 2010; Gu et al., 2015), or (2) adding an enhanced diffusivity values term to account for other sources of turbulence such as horizontal currents and advection (Subin et al., 2012; Wang et al., 2019). Thus, we set MIXFACT as a tunable parameter to observe the effect of eddy diffusivity on lake thermal properties.

The model time step was set to 30 min to adequately resolve diurnal variations in lake temperature. Hourly data were linearly interpolated to obtain input values at a 30-min time step. The lake temperature outputs were calculated and averaged to daily values. Yearly DJF, MAM, JJA, and SON temperatures were determined by averaging the daily lake temperature values during those months. The whole-lake temperature is weighted based on lake area per lake depth. For future projections, lake thermal profiles generated by the lake energy balance model were further averaged every decade to remove short-term variability in the lake temperatures.

3.2.2. Model calibration and validation

To calibrate the lake energy balance model, an 800-member ensemble of simulations was generated across 100 possible combinations of CDRN ($5 \times 10^{-4} – 3 \times 10^{-3}$) and ETA values (0.01–0.50 m^{-1}) via hypercube sampling method with MIXFACT of 1, 5, 10, 50, 100, 250, 500, and 1000. Modeled lake temperatures were evaluated using observed daily average lake temperatures where available. The lake temperature observation from the north end is available between August 21, 2017 to August 7, 2018, while the observation from the south end is available from August 30, 2016 to August 15, 2017 and from August 26, 2017 to August 11, 2018. The optimal combination of model parameters was chosen based on the root mean square error between simulations and observations (RMSE):

$$\text{RMSE} = \sqrt{\frac{\sum(y_{i,obs} - y_{i,pred})^2}{n}}$$

where $y_{i,obs}$ is the i^{th} lake temperature observation, $y_{i.pred}$ is the i^{th} modeled lake temperature values, $\bar{y}_{obs}$ is the mean of lake temperature observation, the $\bar{y}_{pred}$ is the mean of modeled lake temperatures, and n is total data points. The RMSE varies from the optimal value of 0.

The global optimal simulated temperature is derived from the choice of the parameters that produced the lowest RMSE in both south-end and north-end observations. Due to the limitation of the instrumental lake temperature dataset,themodel wasnotvalidatedbased ondatanotused in the calibration. We also calculated Prediction bias (Bias; unit °C) to measure how far apart the averages of observed vs. modeled outcomes are:

$$\text{Bias} = \frac{\sum(y_{i,obs} - y_{i,pred})}{n}$$

The closer to 0 °C Bias is, the better model performance is. We calculated temperature differences between the model and observation for every depth and time. Then, all difference values were averaged to get the Bias index.

4. Results

4.1. Bias correction of the ERA5-Land climate variables

A comparison of the original ERA5-Land climate variables, quantile-mapped ERA5-Land values, and meteorological observations during the overlapping period (2016–2023) is shown in Fig. 2e–h. Overall, seasonal and diurnal patterns of the ERA5-Land variables correspond well with the observed variables, except for surface pressure, for which absolute values differ slightly.

The ERA5-Land T2M reveals a cold bias, particularly during afternoon and night (Fig. 2e). The monthly-averaged ERA5 wind speed is substantially weaker and less variable than observations (Fig. 2g). ERA5-Land relative humidity displays a wet bias, particularly during the austral winter with JJA average temperature 14.70 ± 9.03 % warmer than observed. Quantile mapping substantially improved the biases in reanalysis inputs (Fig. 2e-h) so the quantile-mapped versions were used as inputs for the energy balance model. Note that radiation observations for Sibinacocha are not available but sensitivity tests found better performance using CERES inputs (Figs. S2-S10) than using inputs from the nearest station data, which is 860 m higher in elevation and situated on an ice cap (Supplementary Information).

4.2. Lake energy balance model calibration

The 800-member calibration test showed that the choice of values for the shortwave extinction coefficient (ETA), neutral drag coefficient (CDRN), and the multiplication factor of eddy diffusivity (MIXFACT) parameters can greatly affect the absolute values and thermal structure of the lake temperature outputs. Different combinations of ETA and CDRN resulted in shifts in the absolute modeled lake temperatures, although the seasonal cycle imprinted on the lake surface temperature (LST) was unaffected. If other variables remain unchanged, the modeled whole-lake temperature generally becomes lower throughout the lake when the ETA decreases and/or the CDRN increases. The output temperature becomes less stratified when CDRN increases and vice versa. The seasonal cycle in lake surface temperature is unaffected by the ETA and CDRN, but the magnitude of sub-seasonal variability slightly increases when the ETA is higher. In general, higher ETA and/or lower CDRN lead to a warmer surface and more stratified lake. However, lake stratification and seasonal cycle timing are greatly affected by

varying MIXFACT (Figs. 3a–b and S13). Higher MIXFACT results in more lake mixing, delaying lake warming during austral spring, and weaker and deeper thermocline.

Based on this calibration test, the combination of CDRN = 1.92×10^{-3}, ETA = 0.165 m^{-1}, MIXFACT = 50 yielded the global optimal temperature result (Fig. 3c). The lake energy balance model simulation using this optimal parameter choice yielded a depth-averaged RMSE and Bias for the south (north) end of the lake of 0.456 (0.465) and 0.135 (0.008), respectively (Table 2).

4.3. Lake energy balance model validation

The annual average of the simulated LST using the hourly quantile-mapped ERA5-Land inputs is 9.41 ± 1.10 °C between August 30, 2016 – August11, 2018. This value is almost identical to the annual average of observed LSTs from both the south end (9.61 ± 1.15 °C; $p > 0.1$) and north end (9.49 ± 1.10 °C; August 21, 2017 – August 8, 2018; $p > 0.1$) (Fig. 3). However, modeled lake temperatures are significantly cooler ($p < 0.05$) than the lowermost south-end in situ lake temperature observations, taken from 21.9 m water depth (9.19 ± 0.88 °C), and from the lowermost north-end in situ lake temperature at 27 m depth (8.85 ± 0.83 °C; August 21, 2017 – August 8, 2018). No lake temperature observations are available below 27 m water depth, but our lake model suggests that the average lake temperatures at 60 m and 92 m deep between August 30, 2016 and August 11, 2018 were 7.75 ± 0.33 °C and 7.56 ± 0.22 °C, respectively (Fig. 4). Since lake temperature observations are unavailable beyond 27 m depth, the model's cold bias at greater depth could potentially skew whole-lake temperature estimates, particularly if temperature changes at the surface and greater depths occur at different rates. However, this effect is likely minimal because whole-lake temperature is calculated as a weighted average. Given that deeper depths have smaller surface areas, the whole-lake temperature is predominantly influenced by temperatures from top depths where lake temperature observations

are available. Seasonality and thermal structure in the lake temperature simulation are generally consistent with real-world observations, with peak warming around December to April and lake cooling rapid cooling after June. As in the observations, the simulated lake does not seasonally freeze. The modeled lake is well-mixed during austral winter and early spring (June–September) but stratifies in austral summer and fall. Although we do not have a complete observation of Sibinacocha's thermal structure, the top 27 m temperature-depth profile of the modeled lake particularly resembles the profile of the north-end temperature as both data show a weak stratification during austral spring (Fig. 4a and e).

4.4. Early 21st century lake temperature and evaporation characteristics

Compared to the observed surface air temperature at the Sibinacocha weather station, modeled lake temperature is significantly warmer and fluctuates less sub-seasonally (Fig. 5a–c). Based on the timing of the seasonal cycles, the modeled LST cools and warms around the same time as the surface air temperature. The modeled daily LST (Fig. 5a) indicates a weak cooling trend between 2000 and 2023 at a rate of 0.09 °C/decade ($p < 0.01$) despite a warming trend in the 2-m air temperature (0.20 °C/decade) and observed air temperatures at the Quelccaya Ice Cap (~10 km east, 860 m higher at 5680 m a.s.l.; 0.56 °C/decade between 2004 and 2017; Hardy, 2019), Cusco (~100 km northwest, 1460 m lower at 3400 m a.s.l. 0.74 °C/decade; 2000–2023; NOAA, 2024a), and La Paz (400 km south, 1220 m lower at 3640 m a.s.l.; 0.39 °C/ decade; 2000–2023; NOAA, 2024b). However, the whole-lake temperature suggests no trend between 2000 and 2023 (Fig. 5b). Lake evaporation is highest in June and lowest in October. The model suggests a weak increase in lake evaporation rate of 0.080 mm/day/decade (2000–2023).

4.5. Late-21st century projections of lake temperature and evaporation

Under the SSP2–4.5 and SSP5–8.5 scenarios, long-term air temperature warming rates in the Cordillera Vilcanota are projected to be 0.38 °C/decade and 0.72 °C/decade, respectively (2015–2100) (Fig.6b). These rates are significantly steeper than the early 21st century rate (0.27 °C/decade; 2000–2014). By 2091–2100, annual air temperature anomalies at this site relative to a 2000–2014 reference period (1.98 ± 0.31 °C) are projected to reach 5.2 °C under the SSP2–4.5 scenario (95 % CI [5.1, 5.3]) and 8.3 °C under the SSP5–8.5 scenario (95 % CI [8.1, 8.3]).

Modeled Sibinacocha lake temperatures increase substantially between 2000 and 2100 under the SSP2–4.5 and SSP5–8.5 scenarios (Fig. 6a and c). The rates of LST ensemble mean under the SSP2–4.5 and SSP5–8.5 scenarios are similar to the air temperature rates (0.38 and 0.73 °C/decade between 2015 and 2100, respectively; Fig. 6c). The whole-lake temperature ensemble mean under the SSP2–4.5 (SSP5–8.5) scenario is projected to warm at 0.36 (0.71) °C/decade between 2015 and 2100. By 2091–2100, the yearly averaged whole lake temperatures are projected to increase 2.5–3.0 °C (temperature mean: 11.4 ± 0.1 °C) under the SSP2–4.5 scenario and 5.0–5.9 °C (temperature mean: 14.1 ± 0.3 °C) under the SSP5–8.5 scenario, relative to a 2000–2014 period. Also, the lake is projected to warm unevenly, with a greater increase expected within the top 20 m and austral winter and early spring (Fig. 7). By 2090s, the lake is projected to exhibit weak stratification during austral spring, a period when it was previously well-mixed.

The lake evaporation rates between 2000 and 2014 show high interannual fluctuation with a short-term trend of 0.001 mm/day/year (Fig. 6d). The lake evaporation rate ensemble mean under the SSP2–4.5 (SSP5–8.5) scenario shows a positive trend of 0.005 (0.013) mm/day/ year. By 2090s, the average lake evaporation rate is projected to increase by 0.38–0.45 mm/day under the

SSP2–4.5 scenario and 0.87–1.06 mm/ day under the SSP5–8.5 scenario, relative to their respective 2000–2014 average.

5. Discussion

5.1. Performance of the energy balance model for Lake Sibinacocha

Our selected combination of ETA, CDRN, and MIXFACT captures absolute values, seasonal ranges, seasonal timing and sub-seasonal variability in lake temperatures that are similar to observations. The values of ETA and CDRN themselves are reasonable choices considering Lake Sibinacocha's trophic state index and water transparency (visually observed during many field seasons, e.g., Michelutti et al., 2020) for ETA and observed wind speed and direction relative to Lake Sibinacocha's geographical orientation for CDRN. Our result suggests that the modeled lake becomes less stratified when CDRN increases, potentially due to increased lake evaporation-linked heat loss and increased convective mixing. That said, in the real world, ETA and CDRN are not static but rather can vary spatiotemporally. Such variations are not captured by our model and could potentially explain deviations in modeled and observed lake temperatures at sub-seasonal timescale. However, our results enable us to assess in-lake and meteorological drivers of the lake thermal structure of Lake Sibinacocha beyond the two-year observed period, and to use the model to contextualize future changes.

The lake energy balance model accurately captures the temperature seasonality, timing, magnitude differences, and stratification characteristics. That said, the simulated south-end lake temperature is significantly warmer than observed between March and June 2017 (Figs. 3c and 4e). Simulated temperatures are much closer to observations for the south-end in 2018, and very

similar to the north-end during that time. Possible explanations include improper specification of lake-specific model parameters and features not simulated by a 1-D model. Our model validation is limited by the depth of available observations from Sibinacocha, which are only available to 27 m water depth. Our bathymetric survey shows the lake is 60.9 m deep on average and 92.8 m deep at maximum. The energy balance model was by necessity validated against the upper 27 m, but it is possible that observations from deeper depths would have yielded different optimal ETA, CDRN, and MIXFACT parameter choices, for example if the real-world lake in fact strongly stratifies below 30 m or exhibits spatial variability in stratification due to the presence of glacial meltwater inputs at the north end. That said, the disparity between simulated and observed temperatures varies across seasons and years, so we suggest that uncertainties in south-end temperature variations may also play a role.

Another possible shortcoming of the 1-D lake model for modeling a large and deep lake such as Sibinacocha is the lack of horizontal mass and energy transport. Observed temperature profiles differ slightly between the lake's north and south ends: the north end exhibits weak stratification during the austral spring, while this feature is absent in the south end (Fig. 4a and c). This indicates that horizontal transport may play a role in lake thermal properties. Notably, the simulated lake temperature aligns better with the north end, which is deeper, whereas the south end's profile resembles those of several shallower lakes in the region (Michelutti et al., 2019a; see location in Fig. 1). Thus, inadequately accounting for horizontal energy transport may contribute to the warmer spring temperatures in the simulation.

Implementing a lake water balance model for Lake Sibinacocha may improve the lake temperature simulation as the lake receives glacial meltwater and is controlled by a dam. However, under the current outflow regulation, the dam is unlikely to affect the lake's overall

temperature substantially. The outflow rates are relatively low, peaking in September at 6.27 m^3/s and dropping to 0.37 m^3/s in March (2002–2016; Bello et al., 2023), especially compared to the lake's total volume of 1.7 km^3. Assuming the lake level has been stable over the long period (i.e., balanced inflows and outflows) and the dam is the only outflow source, the estimated residence time of the lake water ranges from 8.5 to 145.6 years based on these flow rates. This relatively long residence time suggests that inflows and outflows have limited influence on the lake's overall temperature dynamics. Additionally, it is worth noting that the pre-dammed outflow rates are similar to those observed after the dam was constructed, ranging from 0.8 to 6.0 m3/s before 1988 (Bello et al., 2023). While changing the seasonality of the outflows may affect lake temperatures, any impact is likely to be localized (i.e., near the dam) since the outflow rates are minimal, compared to the lake volume, and the estimated residence time is long.

However, glaciers in the Cordillera Vilcanota are projected to continue retreating, with the acceleration expected in response to anthropogenic warming (Yarleque et al., 2018; Montoya-Jara et al., 2024). Accelerating glacial melting will undoubtedly result in higher glacial meltwater inflows into the lake, potentially dampening the effect of lake warming caused by increasing radiative forcings. Although no specific studies have been conducted on the glacier connected to the northern part of Sibinacocha, the nearby Suyuparina glacier and the Quelccaya Ice Cap are projected to disappear in 2081 and 2070s, respectively (Montoya-Jara et al., 2024; Yarleque et al., 2018). If the northern glacier disappears, the resulting loss of a major inflow could substantially change the lake's water balance, leading to decreased lake levels and potentially impacting its thermal structure. Further work should investigate how changes in water and glacier balances will affect Lake Sibinacocha's temperature dynamics.

Despite these caveats and the limitations inherent to a 1-D energy balance model, the model still adequately captures the observed timing, duration, and amplitude of the seasonal cycle; the absolute values of lake temperature; the annual average surface temperatures; and the depth of convective mixing (Fig. 3). Therefore, it is reasonable to use the model to examine long-term (annual to decadal) changes in lake thermal properties over time. Given the lack of lake modeling work for South America and for the tropics more generally, the lake temperature simulation is still a useful first step in contextualizing ongoing changes in high alpine lacustrine systems. We next use the model to evaluate long-term changes in lake thermal properties over the 21st centuries (Section 5.2).

5.2. Modeled impacts of anthropogenic warming on lake thermal structure

Given the rapid warming of air temperatures in the high Andes (Fig. 5c), one might expect Andean lakes to also warm rapidly. However, Lake Sibinacocha LST and whole-lake temperature exhibit no significant trend between 2000 and 2023. Note that the simulated lake temperature is independent of temperature change due to potential meltwater input, as the model does not incorporate the glacial input. Lake elevation alone is unlikely to explain the lack of significant early 21st century warming; in fact, a global survey of lake temperatures (O'Reilly et al., 2015) found no relationship between LST warming rates and lake altitude or morphometry (lake mean depth, lake surface area, and lake volume). We suggest that the large amplitude of interannual variability at Sibinacocha masks any trend in LST or whole-lake temperature until the warming signal becomes more substantial in the mid-21st century.

In contrast to no warming during the observational period, warming throughout the water column at Sibinacocha is projected to accelerate during the 21st century as Andean air temperature warming accelerates (Fig. 7). By the end of the 21st century, Lake Sibinacocha whole-lake

temperature is projected to increase between 2.5 °C – 5.9 °C relative to the 2000–2014 mean. These warming rates under the SSP2–4.5 and SSP5–8.5 scenarios are comparable to or even higher than the projected warming rates in many lakes from Europe (Shatwell et al., 2019; Czernecki and Ptak, 2018; Fuso et al., 2021; Lepori and Roberts, 2015), USA (Matsumoto et al., 2019); and worldwide (Woolway and Merchant, 2019; Jansen et al., 2022; Grant et al., 2021). These results imply that, although Lake Sibinacocha's response to climate change has heretofore been muted, as atmospheric warming continues due to increased radiative forcing, Sibinacocha's response will become more similar to other lakes worldwide. Notably, the projected lake temperature increases under both scenarios exceed the range of early 21st century interannual variability.

Increased lake surface temperature due to increased air temperatures and downward longwave radiation will enhance the rate of lake evaporation due to more radiation energy available for evaporation (Woolway et al., 2020; Wang et al., 2018). The lake evaporation rate at Lake Sibinacocha is projected to increase significantly compared to the early 21st century rate. Increased lake evaporation could potentially lead to an increase in local cloud cover (Zhan et al., 2019) which could enhance longwave radiation to the lake beyond what the future scenarios project. However, lake warming also promotes more lake evaporative cooling, which could potentially weaken the relationship between rising air temperatures and lake temperatures (Wang et al., 2018; Tong et al., 2023).

Anthropogenic warming is one of the biggest threats to water resources in the tropical high Andes. Peru especially has already experienced rapid ice mass loss from glaciers and ice caps (Chevallier et al., 2011; Hanshaw and Bookhagen, 2014; Salzmann et al., 2013), shifting of high-altitude fauna (Seimon et al., 2017) and flora (Jameson and Ramsay, 2007), as well as changes in

wetland system dynamics (King et al., 2021). Human-induced warming will also likely amplify the stressors on lake ecosystems. Although the mixing regime at Lake Sibinacocha is projected to remain relatively similar to today, future warming will likely drive shifts in algal communities, which are sensitive to thermal structure regime and lake-level changes (Fritz et al., 2019; Michelutti et al., 2020; Rühland et al., 2015). With continued temperature increases, an overall loss in overall aquatic biodiversity may occur as some species may not be able to adjust to rapid warming. Cold-water fish species such as trout (habitat temperature of 7–18 °C) are particularly vulnerable to warming temperatures, and at Sibinacocha, non-native trout are an important food source for local communities. Lake warming and other limnological changes may reduce the amount of dissolved oxygen in water, which is unfavorable for trout populations. As warming continues in the Andes, suitable habitat for these cold-water fish is expected to decline. This may lead to the elimination of some populations of these fish, with consequences for the ecosystem and the food security of Andean communities.

6. Conclusions

Despite its high altitude and cold temperatures, our model suggests that Lake Sibinacocha has yet to see a significant increase in surface or whole-lake temperatures, likely due to large interannual variability. However, future anthropogenic warming under both moderate and high radiative forcing scenarios will likely drive Lake Sibinacocha to warm significantly. Lake evaporation will likely increase due to increased energy inputs. Although Lake Sibinacocha is an atypical lake in the tropical Andean highlands due to its exceptional length and depth, our lake modeling results can still serve as a baseline of climate change response for other lakes in the tropical highlands. Large lakes are generally less susceptible to lake temperature change because

they have a larger heat storage capacity than smaller lakes (Rouse et al., 2005). If Lake Sibinacocha indicates a major change in lake temperature and/or a thermal stratification regime, other smaller and shallower lake temperatures in the region are likely at even greater risk of change. Such drastic projected changes within less than a century will almost certainly modify local ecosystems and should be directly considered in climate change adaptation efforts.

Acknowledgements

We thank Douglas R. Hardy (University of Massachusetts Amherst) for the Quelccaya Ice Cap radiation observation dataset, and we are grateful to Preston Sowell and the Crispín Condori de Ocongate family for field logistical support and assistance with bathymetric surveys. This research was funded by NSF-EAR (P2C2) #2103081 to B. Konecky, National Geographic Society Standard Grant #HJ-097R-17 to B. Konecky, and by the International Center of Energy, Environment, and Sustainability (InCEES) at Washington University.

Data availability

The 1-D lake energy balance model used in this research can be accessed at https://github.com/carriemorrill/lake-model. The GitHub repository for this paper can be accessed at https://github.com/njsaelim/Sibinacocha-lake-modeling.

References

Adrian, R., O'Reilly, C.M., Zagarese, H., Baines, S.B., Hessen, D.O., Keller, W.,Livingstone, D.M., Sommaruga, R., Straile, D., Van Donk, E., Weyhenmeyer, G.A.,Winder, M., 2009. Lakes as sentinels of climate change. Limnol. Oceanogr. 54 (6 PART 2), 2283–2297. https://doi.org/10.4319/lo.2009.54.6_part_2.2283.

Baied, C.A., Wheeler, J.C., 1993. Evolution of high Andean Puna ecosystems: environment, climate, and culture change over the last 12,000 years in the Central Andes. Mt. Res. Dev. 13 (2), 145–156. https://doi.org/10.2307/3673632.

Bello, C., Suarez, W., Drenkhan, F., Vega- Jácome, F., 2023. Hydrological impacts of damregulation for hydropower production: the case of Lake Sibinacocha, Southern Peru. J. Hydrol. Reg. Stud. 46, 101319. https://doi.org/10.1016/j.ejrh.2023.101319.

Benito, X., Benito, B., Vélez, M.I., Salgado, J., Schneider, T., Giosan, L., Nascimiento, M.,2022. Human practices behind the aquatic and terrestrial ecological decoupling to climate change in the tropical Andes. Sci. Total Environ. 826, 154115.https://doi.org/10.1016/j.scitotenv.2022.154115.

Buytaert, W., Moulds, S., Acosta, L., De Bièvre, B., Olmos, C., Villacis, M., Tovar, C., Verbist, K.M.J., 2017. Glacial melt content of water use in the tropical Andes. Environ. Res. Lett. 12 (11). https://doi.org/10.1088/1748-9326/aa926c.

Chevallier, P., Pouyaud, B., Suarez, W., Condom, T., 2011. Climate change threats to environment in the tropical Andes: glaciers and water resources. Reg. Environ. Chang. 11 (Suppl. 1), 179–187. https://doi.org/10.1007/s10113-010-0177-6.

Czernecki, B., Ptak, M., 2018. The impact of global warming on lake surface water temperature in Poland -the application of empirical-statistical downscaling, 1971-2100. J. Limnol. 77 (2), 330–348. https://doi.org/10.4081/jlimnol.2018.1707.

Danabasoglu, G., 2019a. NCAR CESM2 Model Output Prepared for CMIP6 CMIPHistorical. Earth System Grid Federation. https://doi.org/10.22033/ESGF/CMIP6.7627.

Danabasoglu, G., 2019b. NCAR CESM2 Model Output Prepared for CMIP6 ScenarioMIPssp245. Earth System Grid Federation. https://doi.org/10.22033/ESGF/CMIP6.7748.

Danabasoglu, G., 2019c. NCAR CESM2 Model Output Prepared for CMIP6 ScenarioMIPssp585. Earth System Grid Federation. https://doi.org/10.22033/ESGF/CMIP6.7768.

Dee, S.G., Morrill, C., Kim, S.H., Russell, J.M., 2021. Hot air, hot lakes, or both? Exploring mid-Holocene African temperatures using proxy system modeling. J. Geophys. Res. Atmos. 126 (10), 1–23. https://doi.org/10.1029/2020JD033269.

Doyle, K.L., Zahler, P., Chutas, C.A., 2003. Biodiversity and the Case for Preservation of the Sibinacocha Watershed Biodiversidad y una recomendación para la conservación de la cuenca del lago. 4(Young 1997), pp. 43–47.

Fritz, S.C., Benito, X., Steinitz-Kannan, M., 2019. Long-term and regional perspectives on recent change in lacustrine diatom communities in the tropical Andes.J. Paleolimnol. 61 (2), 251–262. https://doi.org/10.1007/s10933-018-0056-6.

Fuso, F., Casale, F., Giudici, F., Bocchiola, D., 2021. Future hydrology of the cryospheric driven Lake Como catchment in Italy under climate change scenarios. Climate 9 (1),1–24. https://doi.org/10.3390/cli9010008.

Gao, Z., Wang, L., Bi, X., Song, Q., Gao, Y., 2012. A simple extension of "an alternative approach to sea surface aerodynamic roughness" by Zhiqiu Gao, Qing Wang, and Shouping Wang. J. Geophys. Res. Atmos. 117 (16), 1–8. https://doi.org/10.1029/2012JD017478.

Grant, L., Vanderkelen, I., Gudmundsson, L., Al, E., 2021. Attribution of global lake systems change to anthropogenic forcing. Nat. Geosci. 14, 849–854. https://doi.org/10.4324/9780203995686-17.

Gu, H., Jin, J., Wu, Y., Ek, M.B., Subin, Z.M., 2015. Calibration and validation of lake surface temperature simulations with the coupled WRF-lake model. Clim. Chang.129, 471–483. https://doi.org/10.1007/s10584-013-0978-y.

Hanshaw, M.N., Bookhagen, B., 2014. Glacial areas, lake areas, and snow lines from 1975 to 2012: status of the cordillera vilcanota, including the Quelccaya Ice Cap, northern Central Andes, Peru. Cryosphere 8 (2), 359–376. https://doi.org/10.5194/tc-8-359-2014.

Hardy, D.R., 2019. Quelccaya Ice Cap Radiation Data, 2010–2012 Hourly Irradiance Average.

Heino, J., Alahuhta, J., Bini, L.M., Cai, Y., Heiskanen, A.-S., Hellsten, S., Kortelainen, P., Kotamäki, N., Tolonen, K.T., Vihervaara, P., Vilmi, A., Angeler, D.G., 2021. Lakes in the era of global change: moving beyond single-lake thinking in maintaining biodiversity and ecosystem services. Biol. Rev. 96, 89–106. https://doi.org/10.1111/brv.12647.

Henderson-Sellers, B., 1985. New formulation of eddy diffusion thermocline models. Appl. Math. Model. 9 (6), 441–446. https://doi.org/10.1016/0307-904X(85)90110-6.

Hostetler, S.W., Bartlein, P.J., 1990. Simulation of lake evaporation with application to modeling lake level variations of Harney-Malheur Lake, Oregon. Water Resour. Res.26 (10), 2603–2612. https://doi.org/10.1029/WR026i010p02603.

Jameson, J.S., Ramsay, P.M., 2007. Changes in high-altitude Polylepis forest cover and quality in the Cordillera de Vilcanota, Perú, 1956-2005. Biol. Conserv. 138 (1–2),38–46. https://doi.org/10.1016/j.biocon.2007.04.008.

Jansen, J., Woolway, R.I., Kraemer, B.M., Albergel, C., Bastviken, D., Weyhenmeyer, G.A., Marcé, R., Sharma, S., Sobek, S., Tranvik, L.J., Perroud, M., Golub, M., Moore, T. N., Råman Vinnå, L., la Fuente, S., Grant, L., Pierson, D.C., Thiery, W., Jennings, E.,2022. Global increase in methane production under future warming of lake bottom waters. Glob. Chang. Biol. 28 (18), 5427–5440. https://doi.org/10.1111/gcb.16298.

Kalff, J., 2002. Limnology: inland water ecosystems, Vol. 592. Prentice Hall, New Jersey.

King, C., Michelutti, N., Meyer-Jacob, C., Bindler, R., Tapia, P., Grooms, C., Smol, J.P., 2021. Diatoms and other siliceous indicators track the ontogeny of a “bofedal” (Wetland) ecosystem in the peruvian Andes. Botany 99 (8), 491–505. https://doi.org/10.1139/cjb-2020-0196.

Kirillin, G., 2010. Modeling the impact of global warming on water temperature and seasonal mixing regimes in small temperate lakes. Boreal Environ. Res. 15 (2),279–293.

Kraemer, B.M., Anneville, O., Chandra, S., Dix, M., Kuusisto, E., Livingstone, D.M., Rimmer, A., Schladow, S.G., Silow, E., Sitoki, L.M., Tamatamah, R., Vadeboncoeur, Y., McIntyre, P.B., 2015. Strati Fi cation responses to climate change. Geophys. Res. Lett. 42, 4981–4988. https://doi.org/10.1002/2015GL064097.

Kronenberg, M., Schauwecker, S., Huggel, C., Salzmann, N., Drenkhan, F., Frey, H., Giráldez, C., Gurgiser, W., Kaser, G., Juen, I., Suarez, W., Hernández, J.G., Sanmartín, J.F., Ayros, E., Perry, B., Rohrer, M., 2016. The projected precipitation reduction over the Central Andes may severely affect Peruvian glaciers and hydropower production. Energy Procedia 97, 270–277. https://doi.org/10.1016/j.egypro.2016.10.072.

Labaj, A.L., Michelutti, N., Smol, J.P., 2018. Annual stratification patterns in tropical mountain lakes reflect altered thermal regimes in response to climate change. Fundam. Appl. Limnol. 191 (4), 267–275. https://doi.org/10.1127/fal/2018/1151.

Lawrence, M.G., 2005. The relationship between relative humidity and the dewpoint temperature in moist air: a simple conversion and applications. Bull. Am. Meteorol. Soc. 86 (2), 225–233. https://doi.org/10.1175/BAMS-86-2-225.

Lepori, F., Roberts, J.J., 2015. Past and future warming of a deep European lake (Lake Lugano): what are the climatic drivers? J. Great Lakes Res. 41 (4), 973–981. https://doi.org/10.1016/j.jglr.2015.08.004.

Martynov, A., Sushama, L., Laprise, R., 2010. Simulation of temperate freezing lakes by one-dimensional lake models: performance assessment for interactive coupling with regional climate models. Boreal Environ. Res. 15, 143–164.

Matsumoto, K., Tokos, K.S., Rippk, J., 2019. Climate projection of Lake Superior under a future warming scenario. J. Li 78 (3). https://doi.org/10.4081/jlimnol.2019.

Michelutti, N., Wolfe, A.P., Cooke, C.A., Hobbs, W.O., Vuille, M., Smol, J.P., 2015. Climate change forces new ecological states in tropical Andean lakes. PLoS One 10 (2), 1–10. https://doi.org/10.1371/journal.pone.0115338.

Michelutti, N., Sowell, P., Tapia, P.M., Grooms, C., Polo, M., Gambetta, A., Ausejo, C., Smol, J.P., 2019a. A pre-Inca pot from underwater ruins discovered in an Andean lake provides a sedimentary record of marked hydrological change. Sci. Rep. 9 (1), 1–10. https://doi.org/10.1038/s41598-019-55422-1.

Michelutti, N., Tapia, P.M., Labaj, A.L., Grooms, C., Wang, X., Smol, J.P., 2019b. A limnological assessment of the diverse waterscape in the Cordillera Vilcanota, Peruvian Andes. Inland Waters 9 (3), 395–407. https://doi.org/10.1080/20442041.2019.1582959.

Michelutti, N., Tapia, P.M., Grooms, C., Labaj, A.L., Smol, J.P., 2020. Differing limnological responses to late Holocene climate variability in the differing limnological responses to late Holocene climate variability in the Cordillera Vilcanota, Peruvian Andes. J. Paleolimnol. May. https://doi.org/10.1007/s10933-020-00127-z.

Montoya-Jara, N., Loayza, H., Gutierrez-Rosales, R.O., Bueno, M., Quiroz, R., 2024. Estimation of glacier outline and volume changes in the vilcanota range snow-capped mountains, Peru, using temporal series of landsat and a combination of satellite radar and aerial LIDAR images. Remote Sens. 16 (20), 3901. https://doi.org/10.3390/rs16203901.

Morrill, C., Meador, E., Livneh, B., Liefert, D.T., Shuman, B.N., 2019. Quantitative model-data comparison of mid-Holocene lake-level change in the central Rocky Mountains. Clim. Dyn. 53 (1–2), 1077–1094. https://doi.org/10.1007/s00382-019-04633-3.

Muñoz Sabater, J., 2019. ERA5-Land Hourly Data from 1950 to Present. Copernicus Climate Change Service (C3S) Climate Data Store (CDS). https://doi.org/10.24381/cds.e2161bac (Accessed on 25 October 2024).

NASA/METI/AIST/Japan Spacesystems and U.S./Japan ASTER Science Team, 2019.ASTER Global Digital Elevation Model V003 [Data set]. NASA EOSDIS LandProcesses Distributed Active Archive Center. https://doi.org/10.5067/ASTER/ASTGTM.003. Accessed 2020-01-10 from.

NOAA, 2024a. Weather Data from Cusco, Peru. https://www.ncdc.noaa.gov.

NOAA, 2024b. Weather Data from La Paz, Bolivia. https://www.ncdc.noaa.gov.

O'Reilly, C.M., Rowley, R.J., Schneider, P., Lenters, J.D., Mcintyre, P.B., Kraemer, B.M., 2015. Rapid and highly variable warming of lake surface waters around the globe. Geophys. Res. Lett. 42, 1–9. https://doi.org/10.1002/2015GL066235.

Rabatel, A., Francou, B., Soruco, A., Gomez, J., Cáceres, B., Ceballos, J.L., Basantes, R., Vuille, M., Sicart, J.E., Huggel, C., Scheel, M., Lejeune, Y., Arnaud, Y., Collet, M., Condom, T., Consoli, G., Favier, V., Jomelli, V., Galarraga, R., Wagnon, P., 2013. Current state of glaciers in the tropical Andes: a multi-century perspective on glacier evolution and climate change. Cryosphere 7 (1), 81–102. https://doi.org/10.5194/tc-7-81-2013.

Romatschke, U., Medina, S., Houze, R.A., 2010. Regional, seasonal, and diurnal variations of extreme convection in the South Asian region. J. Clim. 23 (2), 419–439. https://doi.org/10.1175/2009JCLI3140.1.

Rouse, W.R., Oswald, C.J., Binyamin, J., Spence, C., Schertzer, W.M., Blanken, P.D., Bussières, N., Duguay, C.R., 2005. The role of northern lakes in a regional energy balance. J. Hydrometeorol. 6 (3), 291–305. https://doi.org/10.1175/JHM421.1.

Rühland, K.M., Paterson, A.M., Smol, J.P., 2015. Lake diatom responses to warming: reviewing the evidence. J. Paleolimnol. 54, 1–35. https://doi.org/10.1007/s10933-015-9837-3.

Rutan, D.A., Kato, S., Doelling, D.R., Rose, F.G., Nguyen, L.T., Caldwell, T.E., Loeb, N.G.,2015. CERES synoptic product: methodology and validation of surface radiant flux. J. Atmos. Ocean. Technol. 32 (6), 1121–1143. https://doi.org/10.1175/JTECH-D-14-00165.1.

Sahoo, G.B., Schladow, S.G., Reuter, J.E., Coats, R., Dettinger, M., Riverson, J., Wolfe, B., Costa-Cabral, M., 2013. The response of Lake Tahoe to climate change. Clim. Chang.116 (1), 71–95. https://doi.org/10.1007/s10584-012-0600-8.

Salzmann, N., Huggel, C., Rohrer, M., Silverio, W., Mark, B.G., Burns, P., Portocarrero, C., 2013. Glacier changes and climate trends derived from multiple sources in the data scarce Cordillera Vilcanota region, southern Peruvian Andes. Cryosphere 7 (1), 103–118. https://doi.org/10.5194/tc-7-103-2013.

Seimon, T.A., Seimon, A., Yager, K., Reider, K., Delgado, A., Sowell, P., Tupayachi, A.,Konecky, B., McAloose, D., Halloy, S., 2017. Long-term monitoring of tropical alpine habitat change, Andean anurans, and chytrid fungus in the Cordillera Vilcanota, Peru: results from a decade of study. Ecol. Evol. 7 (5), 1527–1540. https://doi.org/10.1002/ece3.2779.

SENAMHI, 2024. Weather Data from Sibinacocha and Cusco Weather Stations, Peru. http://senamhi.gob.pe.

Shatwell, T., Thiery, W., Kirillin, G., 2019. Future projections of temperature and mixing regime of European temperate lakes. Hydrol. Earth Syst. Sci. 23 (3), 1533–1551. https://doi.org/10.5194/hess-23-1533-2019.

Shippee, R., 1991. Shippee-Johnson Peruvian Expedition Aerial Film Collection, 1931-1999, Film Collection No. 292. Museum Archive at the Gottesman Research Library.https://data.library.amnh.org/archives/repositories/3/resources/9754. Accessed January 21, 2025.

Subin, Z.M., Riley, W.J., Mironov, D., 2012. An improved lake model for climate simulations: model structure, evaluation, and sensitivity analyses in CESM1. J. Adv.Model. Earth Syst. 4 (2), 1–27. https://doi.org/10.1029/2011MS000072.

Thompson, L.G., Davis, M.E., Mosley-Thompson, E., 1994. Glacial records of global climate: a 1500-year tropical ice core record of climate. Hum. Ecol. 22 (1), 83–95. https://doi.org/10.1007/BF02168764.

Thompson, L.G., Mosley-Thompson, E., Davis, M.E., Zagorodnov, V.S., Howat, I.M., Mikhalenko, V.N., Lin, P.N., 2013. Annually resolved ice core records of tropical climate variability over the past ~1800 years. Science 340 (6135), 945–950. https://doi.org/10.1126/science.1234210.

Tong, Y., Feng, X. Wang, Pi, X., Xu, W., Woolway, R.I., 2023. Global lakes are warming slower than surface air temperature due to accelerated evaporation. Nat. Water 1, 929–940. https://doi.org/10.1038/s44221-023-00148-8.

Urrutia, R., Vuille, M., 2009. Climate change projections for the tropical Andes using a regional climate model: temperature and precipitation simulations for the end of the21st century. J. Geophys. Res. Atmos. 114 (2), 1–15. https://doi.org/10.1029/2008JD011021.

Vuille, M., 2014. Inter-American Development Bank Environmental Climate Change and Water Resources in the Tropical Andes Mathias Vuille. October. https://doi.org/10.13140/2.1.3846.9124.

Vuille, M., Francou, B., Wagnon, P., Juen, I., Kaser, G., Mark, B.G., Bradley, R.S., 2008.Climate change and tropical Andean glaciers: past, present and future. Earth Sci.Rev. 89 (3–4), 79–96. https://doi.org/10.1016/j.earscirev.2008.04.002.

Wang, W., Lee, X., Xiao, W., Liu, S., Schultz, N., Wang, Y., Zhang, M., Zhao, L., 2018. Global lake evaporation accelerated by changes in surface energy allocation in a warmer climate. Nat. Geosci. 11 (6), 410–414. https://doi.org/10.1038/s41561-018-0114-8.

Wang, F., Ni, G., Riley, W.J., Tang, J., Zhu, D., Sun, T., 2019. Evaluation of the WRF lake module (v1. 0) and its improvements at a deep reservoir. Geosci. Model Dev. 12 (5), 2119–2138. https://doi.org/10.5194/gmd-12-2119-2019.

Winslow, L.A., Leach, T.H., Rose, K.C., 2018. Global lake response to the recent warming hiatus. Environ. Res. Lett. 13 (5). https://doi.org/10.1088/1748-9326/aab9d7.

Woolway, R.I., Merchant, C.J., 2019. Worldwide alteration of lake mixing regimes in response to climate change. Nat. Geosci. 12 (4), 271–276. https://doi.org/10.1038/s41561-019-0322-x.

Woolway, R.I., Kraemer, B.M., Lenters, J.D., Merchant, C.J., O'Reilly, C.M., Sharma, S., 2020. Global lake responses to climate change. Nat. Rev. Earth Environ. 1 (8), 388–403. https://doi.org/10.1038/s43017-020-0067-5.

Woolway, R.I., Sharma, S., Weyhenmeyer, G.A., Debolskiy, A., Golub, M., Mercado-Bettín, D., Perroud, M., Stepanenko, V., Tan, Z., Grant, L., Ladwig, R., Mesman, J.,Moore, T.N., Shatwell, T., Vanderkelen, I., Austin, J.A., DeGasperi, C.L., Dokulil, M.,La Fuente, S., Jennings, E., 2021. Phenological shifts in lake stratification underclimate change. Nat. Commun. 12 (1), 1–11. https://doi.org/10.1038/s41467-021-22657-4.

Woolway, R.I., Denfeld, B., Tan, Z., Jansen, J., Weyhenmeyer, G.A., La Fuente, S., 2022. Winter inverse lake stratification under historic and future climate change. Limnol.Oceanogr. Lett. 7 (4), 302–311. https://doi.org/10.1002/lol2.10231.

Yarleque, C., Vuille, M., Hardy, D.R., Timm, O.E., De la Cruz, J., Ramos, H., Rabatel, A., 2018. Projections of the future disappearance of the Quelccaya Ice Cap in the CentralAndes. Sci. Rep. 8 (1), 1–11. https://doi.org/10.1038/s41598-018-33698-z.

Zhan, S., Song, C., Wang, J., Sheng, Y., Quan, J., 2019. A global assessment of terrestrial evapotranspiration increase due to surface water area change. Earth's Future 7 (3), 266–282. https://doi.org/10.1029/2018EF001066.

Figures

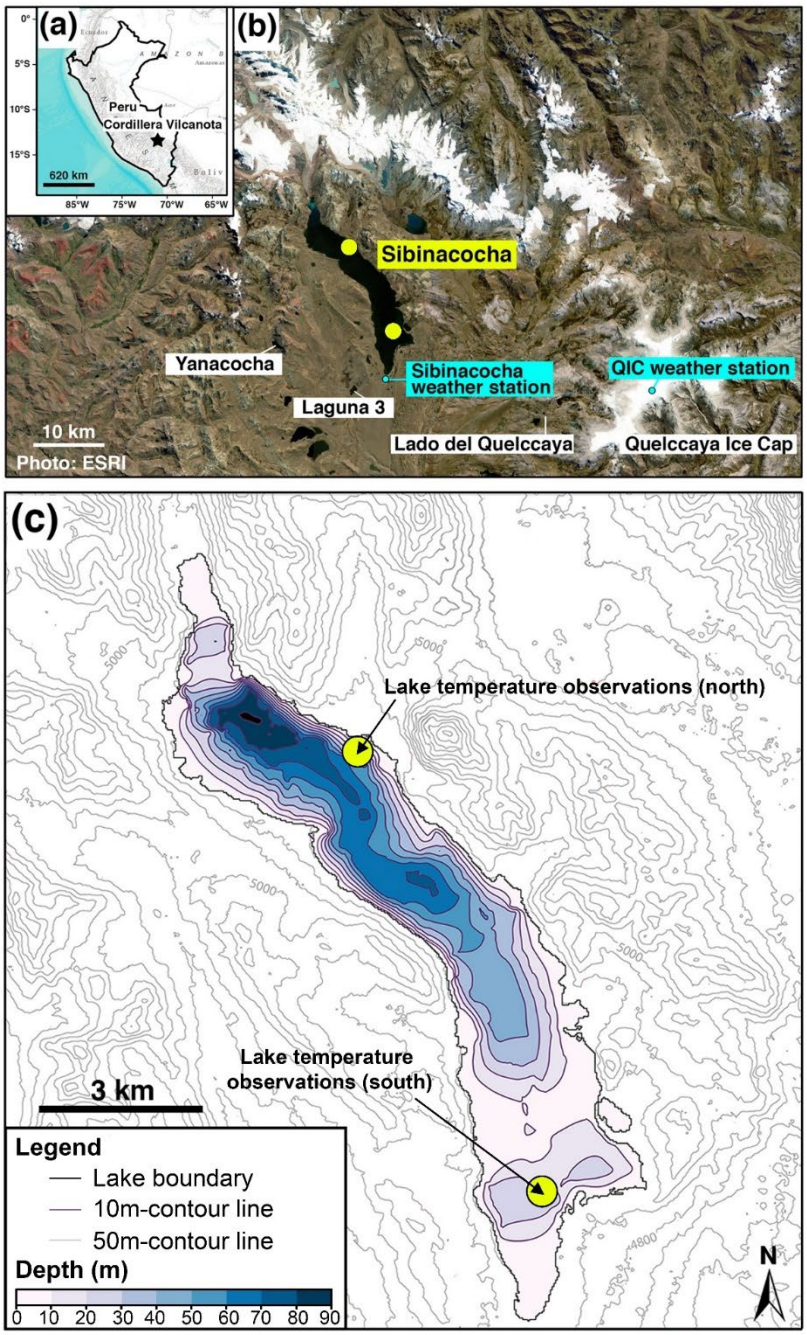

Fig. 1. Study site and bathymetric map of Lake Sibinacocha. (a) Map of Peru denoting the Cordillera Vilcanota (black square; Detail in (b)). (b) The Cordillera Vilcanota with names of lakes and locations of lake temperature and weather station observations discussed in the text. (c)

Bathymetric map of Lake Sibinacocha based on natural neighbor interpolation of sonar data collected in August 2019 and May 2019. Shading depicts lake depth ranging from 0 m to 92.75 m. Purple contour lines within the lake are 10 m-contour lines calculated from lake bathymetry. Gray contour lines on land are 50 m-contour lines based on ASTER Global Digital Elevation Model V003 (NASA/METI/AIST/Japan Spacesystems and U.S./Japan ASTER Science Team, 2019). Yellow circles represent the locations of lake temperature logger data described in Michelutti et al. (2019a).

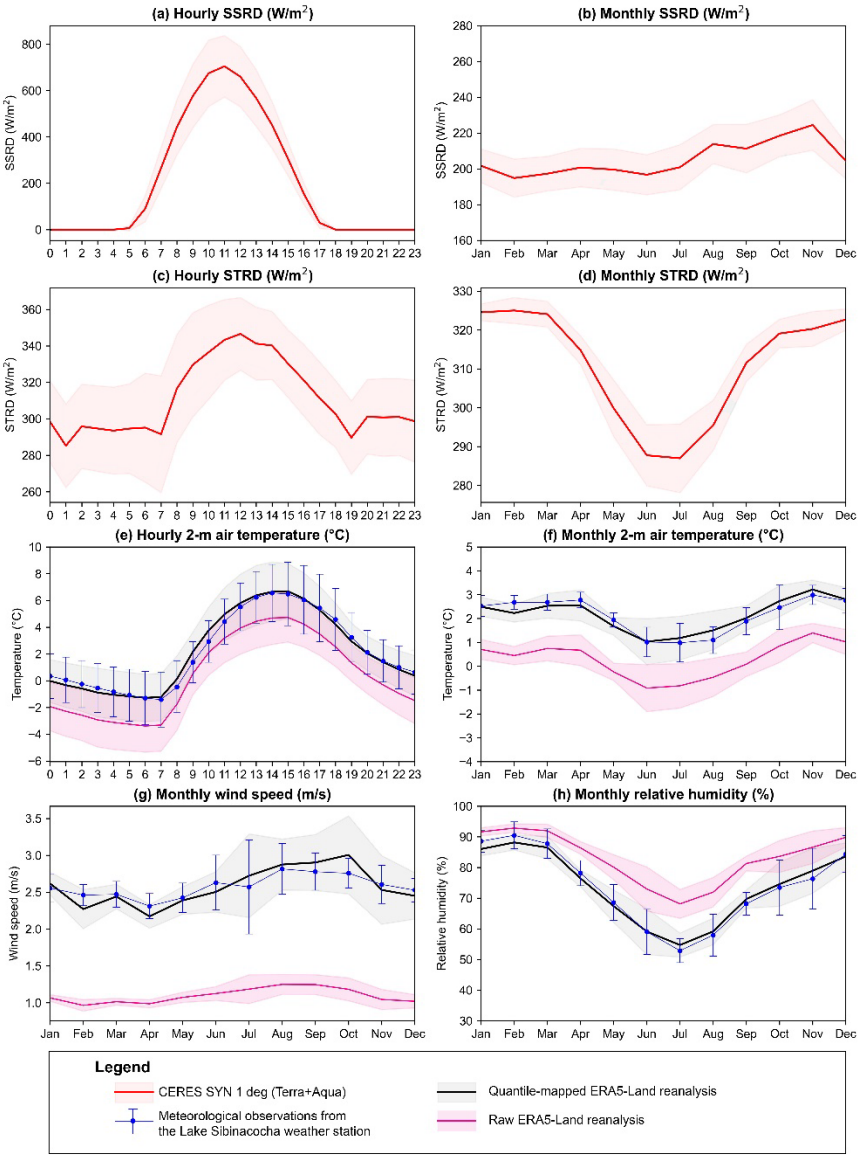

Fig. 2. Hourly and monthly climatologies of raw and quantile-mapped lake model input variables. (a) CERES surface shortwave radiation downwards hourly averages (SSRD; W/m^2). (b) CERES SSRD monthly averages (W/m^2). (c) CERES surface thermal radiation downwards hourly averages (STRD; W/m^2). (d) CERES STRD monthly averages. The red lines and shadings in (a) – (d) are averages between March 2000 and December 2023 and their respective standard deviations. (e) 2-m air temperature (T2M) hourly averages. (f) T2M monthly averages. (g) wind speed monthly averages, and (h) relatively humidity monthly averages. The pink lines

and pink shadings in (e) – (h) are averages and corresponding standard deviations from the raw ERA5-Land dataset (March 2016 – December 2023), while the black lines with gray shadings are the quantile-mapped ERA5-Land variables and their standard deviations. The blue lines with blue error bars are the mean and standard deviation of the observations from the Sibinacocha weather station.

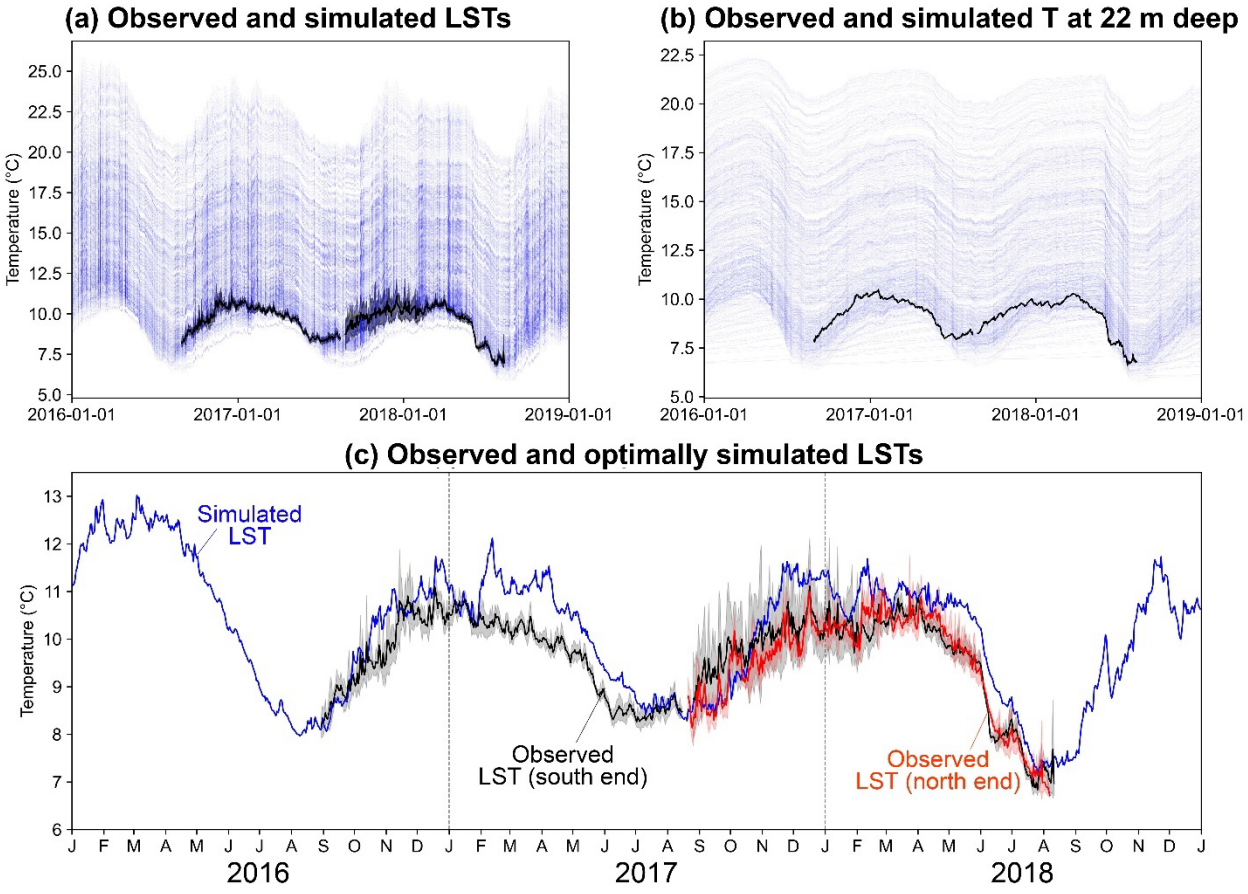

Fig. 3. Observed and modeled daily lake temperatures at Lake Sibinacocha. (a) Observed lake surface temperature (south end; black) and 800-member ensemble of simulated lake surface temperatures with varying parameter choices (blue). (b) As in a, but for temperatures at 22 m water depth. (c) Simulated lake surface temperature using optimal parameter choices (blue) vs.

observed daily lake surface temperatures at Sibinacocha's south end (black) and north end (red). The shadings in the daily mean observations show their respective standard deviations.

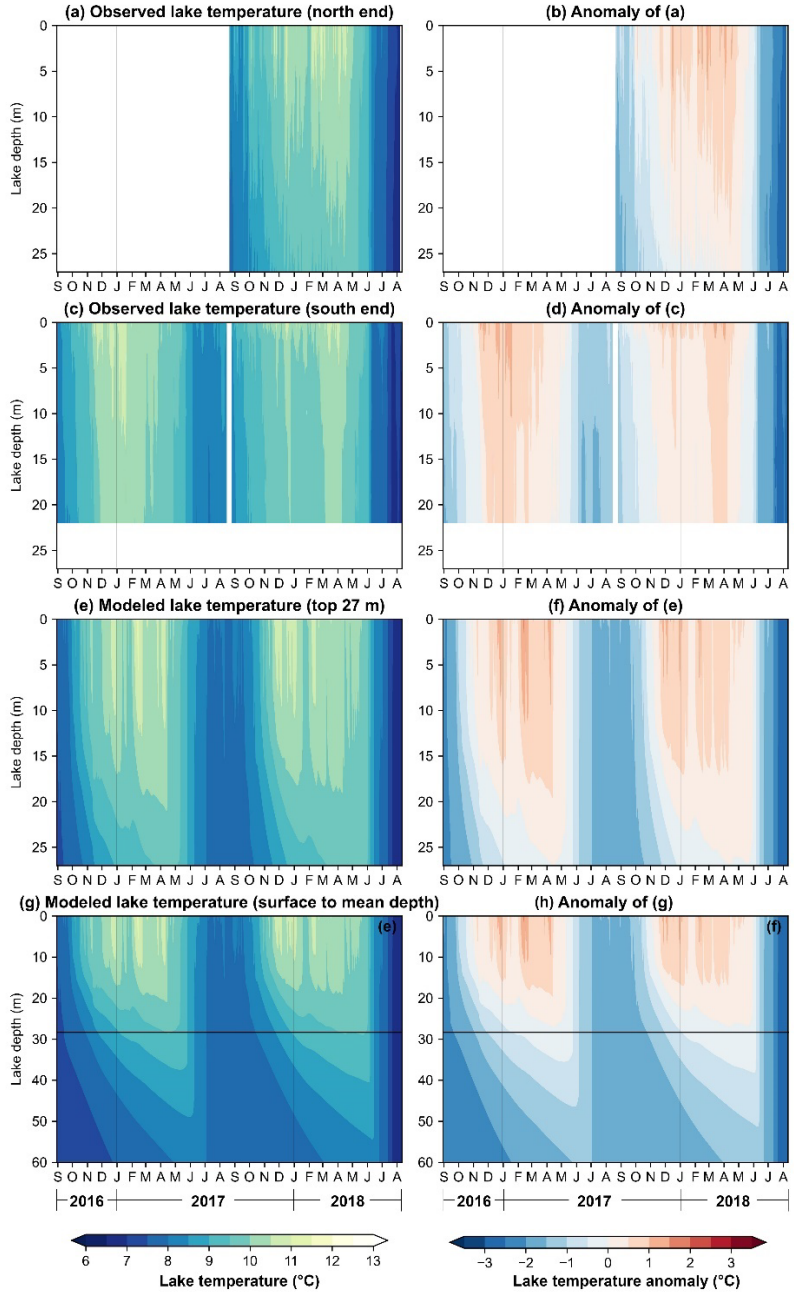

Fig. 4. Observed and modeled lake temperature absolute values and anomalies vs. depth and time. (a) Observed Sibinacocha lake temperature from the north-end station. (b) Temperature anomaly of (a) relative to the mean lake surface temperature. (c) Observed Sibinacocha lake temperature from the south-end station. (d) Temperature anomaly of (c) relative to the mean lake surface temperature. (e) Simulated Sibinacocha lake temperature from 0 to 27 m deep. (f) Temperature anomaly of (e). (g) Simulated Sibinacocha lake temperature from 0 to 60 m deep (i.e., lake mean depth). (h) Temperature anomaly of (g). Anomaly plots (b), (d), (f), and (h) are relative to the mean lake surface temperature of the south-end lake temperature observations. Horizon black lines in (g) and (h) denote 27 m, i.e., the maximum depth of observations and of the values plotted in (a), (b), (e), (f). X-axes are months from September 2016 to August 2018. White color highlights region and time with no data.

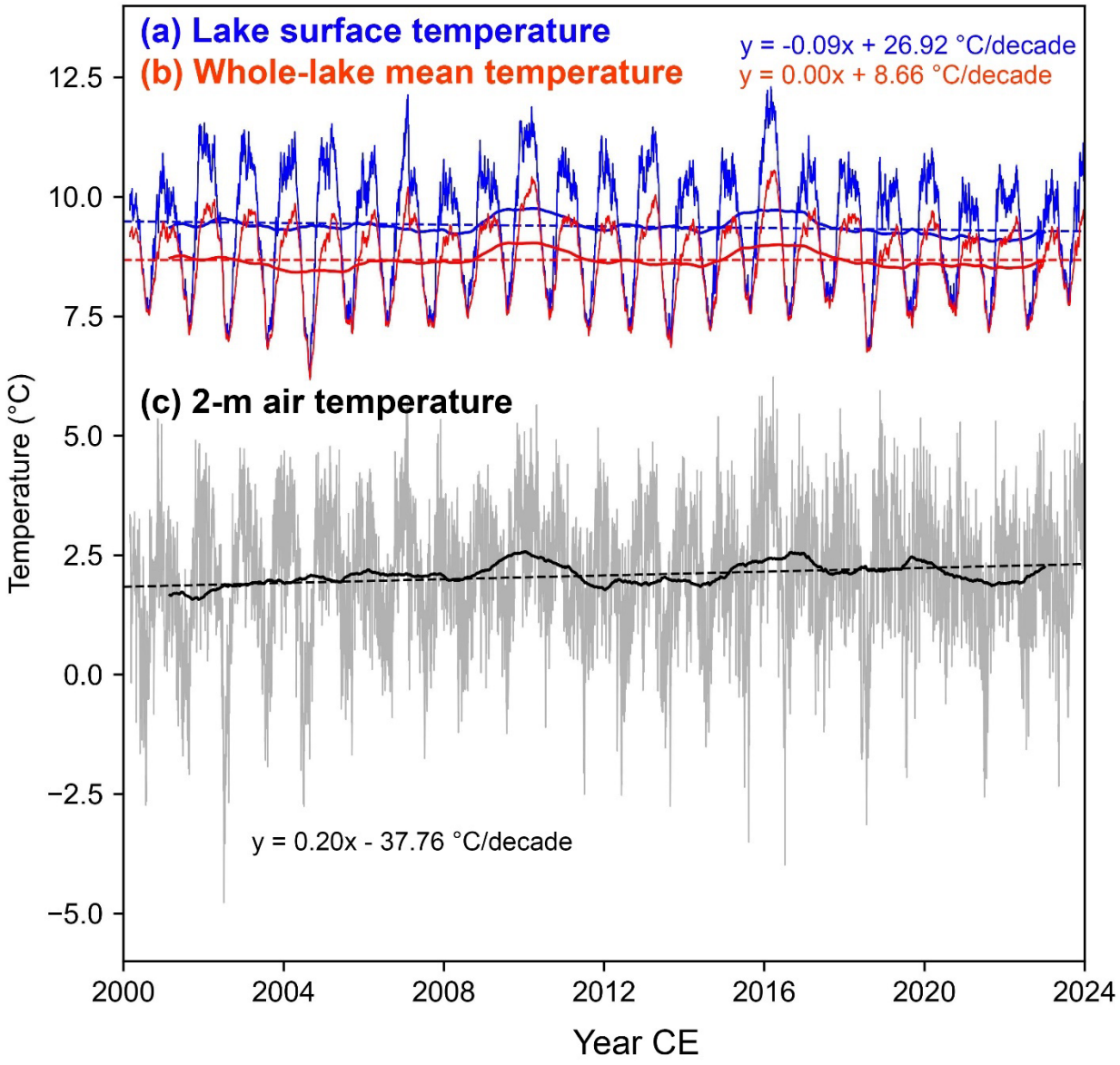

Fig. 5. Whole-lake and surface lake temperatures and air temperatures between 2000 and 2023. (a) Modeled lake surface temperature of Lake Sibinacocha. (b) Modeled whole-lake temperature. (c) 2-m air temperature from quantile-mapped ERA5-Land. The thick lines indicate a running mean of 2 years, while the dashed lines show long-term trends in lake and air temperatures.

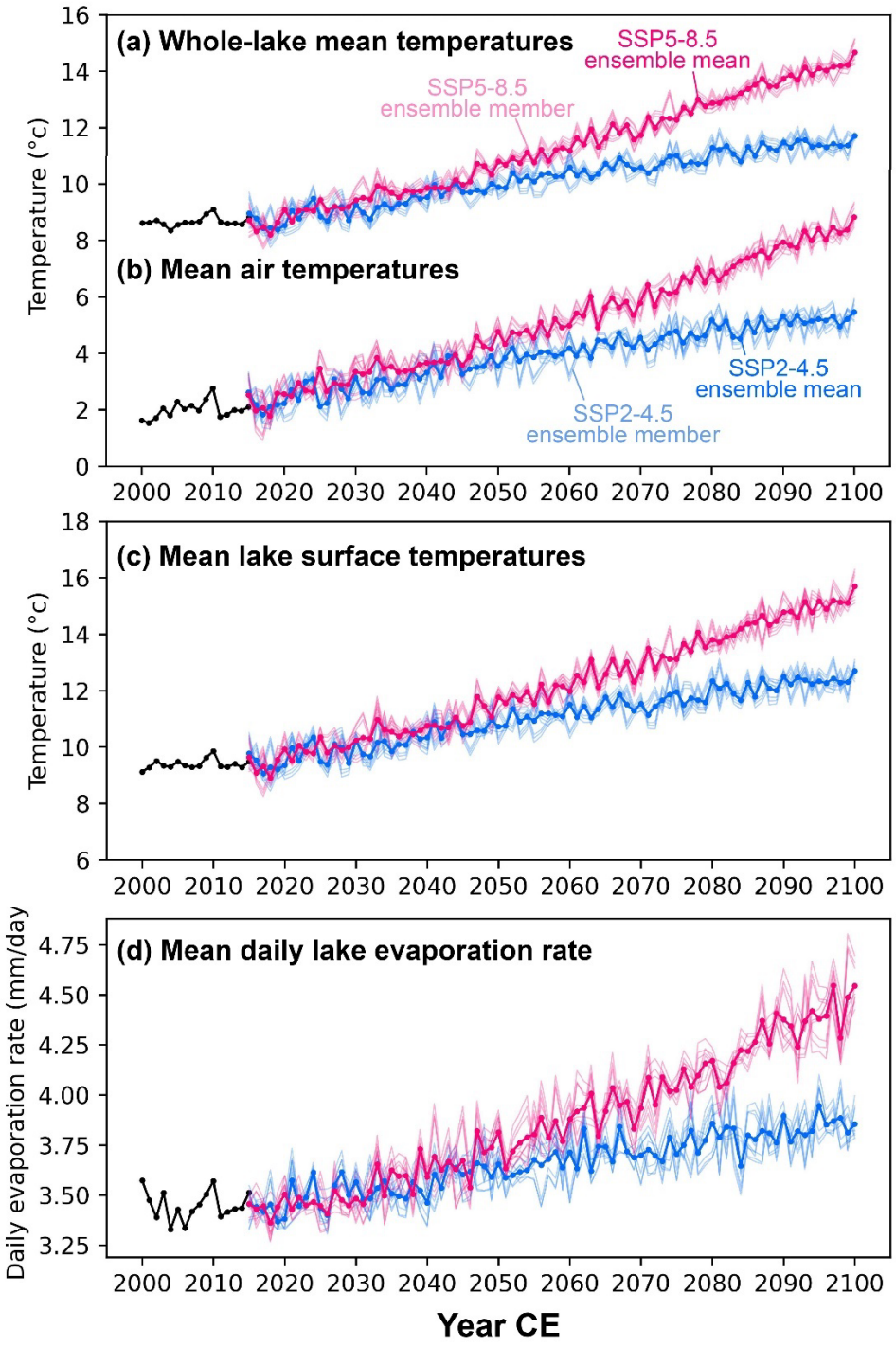

Fig. 6. lake temperature, air temperature, and lake evaporation projections to 2100 CE. (a) Annual mean whole-lake temperatures. (b) Annual mean 2-m air temperatures. (c) Annual mean lake surface temperatures. (d) Annual mean daily evaporation rates. The black lines represent

modeled results based on quantile-mapped ERA5-Land and CERES inputs. Thick blue and pink lines are the modeled results based on CMIP6 CESM ensemble means under the SSP2–4.5 (blue) and SSP5–8.5 (pink) scenarios. The thin lines are mean projections from individual ensemble members.

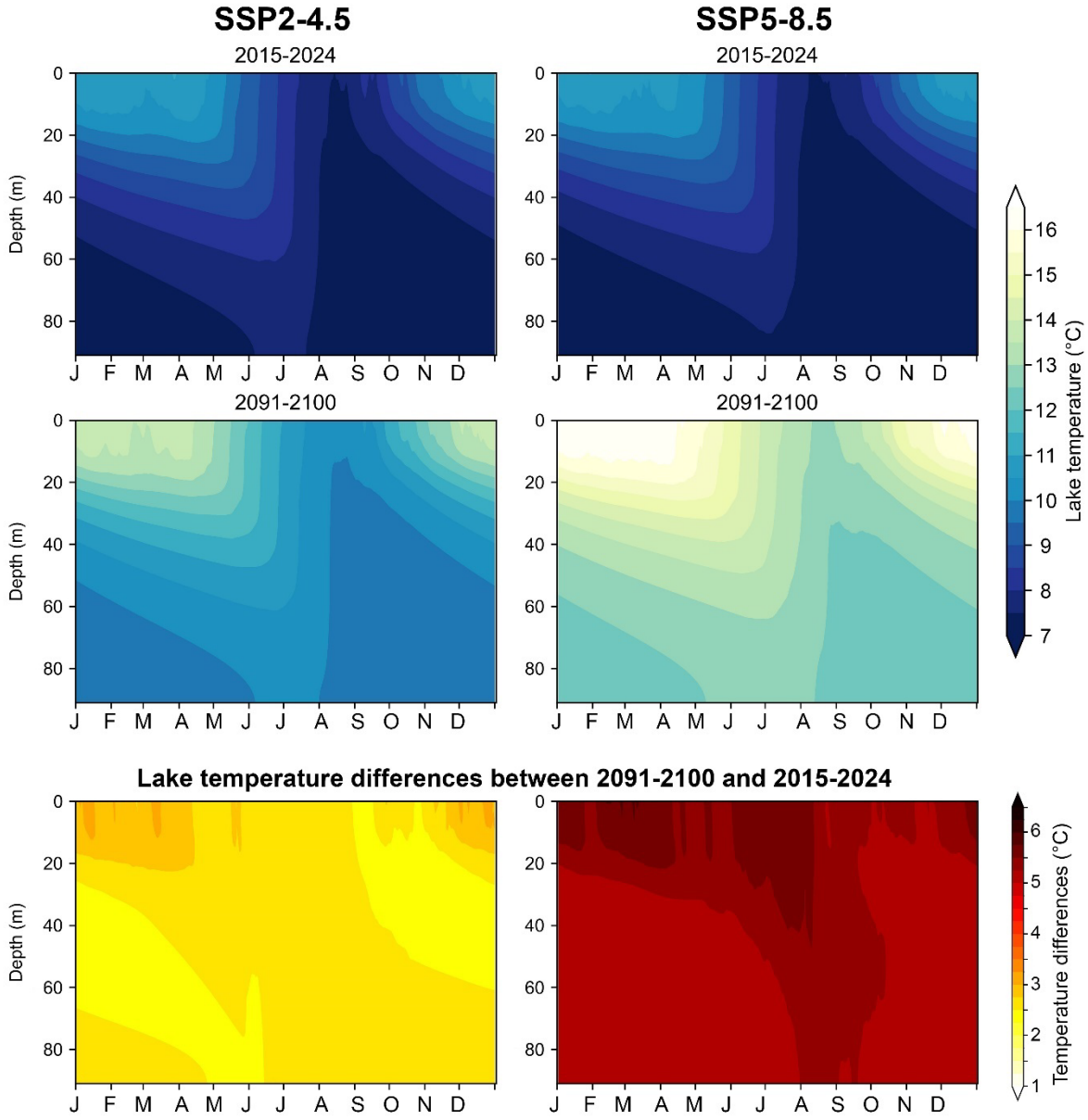

Fig. 7. Projected lake temperatures under SSP2–4.5 and SSP5–8.5 scenarios and lake temperature differences between 2015 and 2024 and 2091–2100. The left (right) column is the outputs produced by the CMIP6 CESM2 SSP2–4.5 (SSP5–8.5) scenario. The top and middle rows are daily-averaged modeled lake temperatures between 2015 and 2014 and 2091–2100. The x-axes are months from January to December and the y-axes show lake depths in m. Colors indicate lake temperature ranging from dark blue (7 °C) to white (16 °C). The bottom row shows modeled lake temperature differences between 2015 and 2024 and 2091–2100. Color indicates lake temperature differences at each specific depth and day of the year.

Tables

Table 1: Limnological and meteorological hourly observations and quantile-mapped reanalysis inputs

Dataset	Location	Time span	Annual average	DJF (Austral summer)	JJA (Austral winter)	Reference
Lake Sibinacocha (4,860 m a.s.l.)						
- Lake temperature (North site; 0 – 27 m deep)	-13.86, -71.02	351 days *(08/21/2017-08/07/2018)*	9.49 ± 1.10°C (LST) 8.85 ± 0.83°C (27 m)	10.29 ± 0.46°C (LST) 9.44 ± 0.22°C (27 m)	7.88 ± 0.68°C (LST) 7.67 ± 0.60°C (27 m)	Michelutti et al. (2019)
- Lake temperature (South site; 0 – 21.9 m deep)	,,	700 days *(08/30/2016 - 08/17/2017, 08/26/2017 – 08/11/2018)*	9.58 ± 1.04°C (LST) 9.17 ± 0.89°C (21.9 m)	10.38 ± 0.52°C (LST) 9.96 ± 0.23°C (21.9 m)	8.15 ± 0.61°C (LST) 7.88 ± 0.54°C (21.9 m)	,,
Sibinacocha weather station (4,880 a.s.l.)						
- Air temperature	-13.92, -71.01	2453 days *(12/1/2016 – 04/21/2019, 08/3/2019 – 12/31/2023)*	2.19 ± 3.36°C	2.66 ± 2.49°C	1.04 ± 4.18°C	SENAMHI (2024)
- Relative humidity	,,	,,	74.13 ± 24.29 %	87.79 ± 16.50 %	56.72 ± 24.03 %	,,
- Wind speed	,,	,,	2.58 ± 2.07 m/s	2.51 ±1.98 m/s	2.69 ± 2.17 m/s	,,
ERA5-Land (reanalysis)						
- Quantile-mapped air temperature	-13.8, -71.1	~23 years *(03/01/2000 – 12/31/2023)*	2.07 ± 3.38°C	2.59 ± 2.66°C	0.87 ± 3.84°C	Sabater (2019)
- Quantile-mapped relative humidity	,,	,,	74.76 ± 23.33 %	86.63 ± 16.84 %	60.08 ± 23.52 %	,,
- Quantile-mapped wind speed	,,	,,	2.50 ± 2.00 m/s	2.33 ± 1.80 m/s	2.68 ± 2.22 m/s	,,
- Surface pressure	,,	,,	56418 ± 202 Pa	56366 ± 204 Pa	56455 ± 191 Pa	,,
CERES (satellite-derived observations)						
- Surface shortwave flux down	-13.5, -71.5	~23 years *(03/01/2000 – 12/31/2023)*	205.44 ± 4.33 W/m^2	200.53 ± 4.04 W/m^2	203.88 ± 7.29 W/m^2	Rutan et al. (2015)
- Surface longwave flux down	,,	,,	310.84 ± 2.77 W/m^2	324.04 ± 1.00 W/m^2	290.10 ± 3.84 W/m^2	

Table 2: Lake model performance and validation (whole lake averaged RMSE and Bias)

Input	CDRN	ETA (m^{-1})	Estimated shortwave extinction depth (m)[a]	MIXFACT	Compare to	Period	RMSE	Bias (ºC)
Quantile-mapped ERA5-Land hourly with CERES radiation.	1.94×10^{-3}	0.16	10.3	50	Daily lake temperature observation from south (north) end	08/30/2016 – 08/11/2018 (08/21/2017 – 08/08/2018)	0.456 (0.465)	0.135 (-0.008)
CMIP6 CESM2 SSP2-4.5	1.94×10^{-3}	0.16	10.3	50	Modeled lake temperature using quantile-mapped ERA5-Land and CERES radiation	01/01/2015-12/31/2019	0.442	0.025
CMIP6 CESM2 SSP5-8.5	”	”	”	”	”	”	0.517	-0.002

[a] Estimated shortwave extinction depth = 1.7/ETA (Kalff, 2011)